Solvent transportation behavior of mechanically constrained agarose gels

Isamu Kaneda* and Sayuri Iwasaki

Department of Food Science and wellness, Rakuno Gakuen University
Bunkyodai Midori-machi, Ebetsu, Hokkaido 069-8501 Japan
Tel/fax +81-11-388-4701
* Correspondance E-mail: kaneda-i@rakuno.ac.jp

Abstract

The mode of transport of solvent from compressed agarose gels that were quenched at various temperatures was investigated. The compression load and the volume of the agarose gels decreased with time during compressive restraint. The decrease in volume was induced by squeezing of the solvent from the gel by compressive restraint. Relaxation of the compression load and the decrease in volume of the gels could be analyzed using a stretched exponential function; moreover, interestingly, both time constants were coupled. It is proposed that relaxation of the compression load was induced by solvent transportation (squeezing out). The hydrogel prepared at just below the sol-gel coexisting temperature (T_{gel}) exhibited distinguishing behavior, characterized by an increase in the rate of the solvent transportation. It is postulated that micro-phase separation occurred in the sample quenched close to T_{gel} due to spinodal decomposition, with consequent formation of relatively large solvent paths in the gel. Turbidity measurements and small angle light scattering data supported this postulate.

Keywords: agarose gel, compression, solvent transportation, quenching temperature

Introduction

The idealized structure of agarose constitutes a disaccharide repeat unit comprising (1→3) linked β-D-galactose and (1→4) linked 3,6-anhydro-α-galactose (Morris 1998). Agarose solutions of sufficiently high concentrations give rise to thermally reversible gels that are slightly turbid and brittle below the gelling temperature. Although the polysaccharides dissolve in water as coils at higher temperatures, they adopt a helical conformation at lower temperature (Arnott et al 1974). The mechanism of formation of the network structure of agarose gel is proposed to proceed as follows: if the concentration of the polysaccharide is sufficiently high, the helices form bundles and the bundles associate to generate a network structure. Electro-microscopic observation of agarose gel demonstrates that the cylindrical fibers of agarose comprise a network structure with a diameter of several tens of nanometers and the mesh size is of the sub-micrometer order (Amici et al 2002; Nordqvist and Vilgis 2011). However, such images have generally been acquired after dehydration of the hydrogels. On the other hand, the micro-scopic image of the swollen agarose gel was observed with confocal laser scanning microscopy (Russ et al 2013). It is reported that the mesh size of 1% agarose gel is about a half micro-meter. Small angle neutron scattering study of the "swollen gels" has revealed the cross-sectional radius of the agarose cylindrical fiber to be a few nm (Boral and Bohidar 2009). From these studies, it is expected that the mesh size of agarose gels is too large to trap water molecules. Therefore, it is quite interesting to study why the solvent never passively flow out from gels?

As is well known, hydrogels swell or de-swell based on the thermodynamic conditions and solvent transport from the inside to the outside of the hydrogel, and vice versa, rather than by simple solvent flow out of the hydrogel. The solvent transportation behavior can be explained in terms of the friction between the gel networks and solvents (Tanaka and Fillmore 1979). A few studies have focused on clarifying the friction within the gel network for chemically crosslinked gels (Tokita and Tanaka 1991; Suzuki and Hara 2001; Fatin-Rougue et al 2003), however, no similar clarification has been provided for polysaccharide gels, which are physically crosslinked gels. Although solvent transportation from edible gels has been extensively studied (Stieger and van de Velde 2013), most of these studies focused on the passive diffusion of the flavor from edible gels (Wang et al 2014). The solvent transportation behavior of the chemically cross-linked hydrogels under mechanical constraint has also been studied (Kneable and Lequeux 1998). The solvent is squeezed out from chemically cross-linked polyelectrolyte gels under compression. However, very little research has been done on physical gels made from polysaccharides from this viewpoint. One phenomenon of interest is the issue of friction between the gel network structure and the solvent, which is appealing from the fundamental perspective as well as for applications.

In this study, we observe the time development of the mechanical load and the volume change for agarose gel under compressive constraint. The relationship between the mechanical response and the volume change, i.e., the mode of solvent transportation from the gel, is also analyzed. Furthermore, to vary the microscopic structure of the gels, agarose gels are prepared at various quenching temperatures, and the effect of the

quenching temperature on the mechanical response and the solvent transportation behavior is investigated.

Materials and Methods

Materials

Agarose type IV (Sigma-Aldrich) was purchased and used without further purification. The sample contained less than 0.25% sulfate. Distilled water (D.W.) was used as a solvent. Sample gels were prepared as follows: agarose powder was dispersed in D.W. and stirred at room temperature for 18 h to allow sufficient swelling. The swollen dispersion was heated at 95 °C for 1 h for complete dissolution. The hot solution was poured into a polycarbonate tube (ϕ = 20 mm) and both ends of the tube were sealed with polyvinylidene chloride film. The tube filled with hot agarose solution was immediately placed in a water bath to control its temperature. After 24 h of quenching in the water bath, the sample gels were squeezed out of the tube and cut to a length of about 20 mm using a razor blade. The cylindrical-shaped gels were immersed in the solvent and incubated at 5 °C for at least 5 days to achieve the equilibrium state before the experiments. The dimensions of the gels (diameter and length) were measured with a caliper just before the experiment. The sample code used herein can be generalized as "XX-G", where "XX" indicates the quenching temperature (T_q).

Phase diagram

For construction of the phase diagram, hot agarose solution of various polymer concentrations (0.5–2.0 wt%) was poured into a glass test tube and sealed with a lid. The test tube was immediately immersed in a water bath, which was kept at 60°C with a large viewing window. After the incubation at 60°C, the samples were cooled until 59°C at a rate of 1°C / h and left at the temperature for 20 h. After naked-eye visual observation, the samples were cooled in the same manner until 20°C. The turbidity of the samples was checked based on the visibility of alphabetical characters (10 pt, printed) placed behind the test tube. When alphabetical characters cannot be clearly seen, the sample was determined as "cloud". The gelling behavior was checked by the tilting method. When the sample did not flow even tilt the 90 degree, it was determined as "gel".

Mechanical property and volume change

For evaluation of the mechanical properties and volume change of the sample, the polymer concentration was fixed at 1.5 wt%. The temporal evolution of the compression load and changes in the shape of the agarose gel were simultaneously monitored using the measuring system shown in Fig.1. The cylindrical-shaped gel was settled in the sample chamber which was filled with the solvent and the temperature was maintained at 30°C by means of a connected circulator. The top and bottom surfaces of the gel were bonded to acrylic resin plates. Compression and monitoring of the compression load were performed with an INSTRON MINI 55 (Instron, USA) instrument. The sample gel was compressed at a rate of 1 mm/s, and the compression was maintained constant when the compression strain reached 0.05. The time development

of the compression load was monitored for 18 h. The side view of the sample was monitored with a CCD camera, and still images were acquired at regular time intervals. The digital images of the samples were analyzed by using image analysis software (Image-J). The width of the sample was measured using the software as shown Fig. 2. Since the gel deformed with a barrel-like shape, the width of five points was measured and the average width (w_m) was obtained. The height of the gel could be determined during the measurements using the INSTRON MINI 55; therefore, the volume (v) of the gel was calculated using Eq. 1.

$$v = \pi\left(\frac{w_m}{2}\right)^2 \cdot h \qquad (1)$$

These measurements were performed at least 3 times.

Optical measurement

The turbidity of the gels prepared at various quenching temperatures was measured by monitoring the transmittance at λ = 540 nm using a photometer. Small angle light scattering (SALS) measurement was performed with a homemade apparatus (Takahashi and Kaneda 2014). A He–Ne laser source (5 mW, λ = 635 nm) (LDU33; Sigma Koki, Tokyo) was used as the light source. The sample solution was sealed in a quartz cell (thickness: 1 mm) and the sample temperature was controlled with a homemade temperature control unit equipped with a circulator. Digital images of the projection of the scattered light on a screen were taken with a digital camera (D-5100; Nikon, Tokyo), and then analyzed with free image analysis software (Image J, and Calib CCD).

Results

Phase diagram in the temperature - concentration plate

Fig. 3 shows the phase diagram for the agarose/water system; the data were obtained during the cooling process. The dotted line and solid line respectively correspond to the cloud temperature line and gelling temperature line. The cloud temperatures were higher than the sol-gel coexisting temperature (T_{gel}) for all the samples. 1.5 wt% agarose gel, which gelled at around 40 °C, was selected for the ensuing experiments. The quenching temperatures were set at 10, 20, 30, 35, and 37 °C; the corresponding samples are denoted 10-G, 20-G, 30-G, 35-G, and 37-G.

Synchronization of relaxation of the compression load and the volume change

Fig. 4 shows the time development of the compression load and compression strain for sample 10-G; the sample was compressed at a speed of 1 mm/s until a strain of 0.05 was achieved, followed by constraint at γ = 0.05. Since the initial height of the sample was about 20 mm, approximately 1 s was required for the compression strain to reach 0.05. The maintenance of the strain (the filled circles in Fig. 4) shows that the

strain was well controlled. On the other hand, the compression load (the open circles in Fig. 4) decreased slightly over time after the peak time. For in-depth evaluation of the decay behavior, a plot of the time development of the compression load was created using the point at which the strain reached 0.05 as time zero. Furthermore, the temporal evolution of the volume change was also plotted. For ease of comparison across samples, the volume change was converted to a relative value using Eq. 2.

$$V(t) = \frac{v(t)}{v_0} \qquad (2)$$

where v(t) and v_0 are the volume of the gel at time "t" and the volume at time zero, respectively. Fig. 5 shows the plots for 10-G (a: the left plate) and 37-G (b: the right plate) as typical examples. It is clear that L(t), the time development of the compression load, and V(t) decayed exponentially. Therefore, the data were subjected to analysis using an empirical stretched exponential function (Eqs. 3 and 4).

$$L(t) = L_0 \exp\left(-\left(\frac{t}{\tau_M}\right)^{\alpha}\right) + L_r \qquad (3)$$

$$V(t) = V_0 \exp\left(-\left(\frac{t}{\tau_V}\right)^{\beta}\right) + V_r \qquad (4)$$

where L_0 and V_0 are the relaxation intensities for the compression load and volume change, respectively; τ_M and τ_V are the time constants of the decay for the compression load and volume change; L_r and V_r are the residue compression load and volume, respectively, and α and β are the respective power indices for each function. The solid lines in Fig. 5 are the best fit results of the analysis using Eqs. 3 and 4; the results of these analyses for all samples are listed in Tables 1 and 2.

It should be noted that the relaxation of the compression load is synchronized with the decay of the gel volume in Fig. 5. Although Fig. 5 shows data for representative samples, a similar tendency was observed for all samples (see Tables 1 and 2). It is clear that the volume decrease is due to de-swelling of the gel in response to the mechanical constraint, i.e., the solvent was squeezed out of the gel due to compression. Because the mechanical relaxation was synchronous with the de-swelling behavior, it is deduced that both parameters are strongly related to each other.

Influence of the quenching temperature

The dependence of τ_M and τ_V on T_q is shown in Fig. 6. It is clear that T_{gel} is approached at higher T_q, thus, the values of τ_M and τ_V decrease. The decrease in τ_V at higher temperatures indicates that the solvent was squeezed out of the gel at a faster rate. These results indicate that the solvent channels expanded as T_q approached T_{gel}. Fig. 7 shows the change in (L_0 + L_r), i.e., the instantaneous load at γ = 0.05, as a function of T_q. This values is also related to T_{gel}, i.e., the compression load decreased when T_q was close to T_{gel}. This means the microscopic structure of the gel changed depending on T_q. To evaluate the changes in the

microscopic structure of the gels, select optical characteristics were investigated. Fig. 8 shows the change in the transmittance of visible light (λ = 540) through the gels as a function of the quenching temperature. The observed trend was similar to those presented in Figs. 6. The decrease in the transmittance for the gels quenched near T_{gel} is indicative of the formation of relatively large scattering bodies in these gels. The scattering profiles of all samples are shown in Fig. 9. Defined peaks (q_m) are evident in the scattering profiles of samples 30-G, 35-G, and 37-G, and the peak height follows the order: 37-G > 35-G > 30-G. It is reported that the reciprocal of q_m is the characteristic length of concentration fluctuation, ξ, in a phase separation system (de Gennes 1979). Given that the value of q_m is about 0.0007 nm^{-1} for these samples, the size of the concentration fluctuation is estimated to be about 1500 nm. This result is consistent with those of the turbidity measurements (Fig. 9), i.e., the strong scattering intensities are derived from the large structures formed in these samples. On the other hand, the samples (10-G and 20-G) quenched at temperatures far below T_{gel} show broad peaks in the relatively high q region, which indicates that the size of the structure is small and there is a distribution of sizes.

Discussion

Firstly, the compression load relaxation behavior is discussed. It is reported that the stress relaxation behavior of agarose gel shows a relaxation component up to 104 s, followed by a plateau region (Watase and Nishinari 1983; Hanazaki et al 2013). In this study, the mechanical relaxation time (τ_M) of the samples, which were quenched below 20°C, were 94.0 ± 29.0 s for 10-G and 97.7 ± 15.5 s for 20-G. There values are consistent with the results of prior studies mentioned above. The relaxation mechanism is described as relaxation of the entangled polysaccharide chains or re-arrangement of the network structures (Watase and Nishinari 1983). However, conclusive evidence of these phenomena has never been documented. Nakamura (2001) and coworkers reported interesting findings in their evaluation of the mechanical relaxation of gellan gel, which is a polysaccharide hydrogel similar to agarose gel. Compression of gellan gel at a compression speed of 1 mm/s induced gel fracture under relatively high compression strain; however, when the compression speed was sufficiently slow (for example 10^{-3} mm/s), the gel deformed in a seat shape without any macroscopic cracks. Although this phenomenon was attributed to rearrangement of the three-dimensional array of the network structure formed by hydrogen-bonding under very slow application of deformation stress, if such a gel is deformed in a very short period and the deformation rate is low, the gel may behave as an elastic body. Therefore, it is unlikely that the network structure of agarose gels completely relax in 10^2 s under deformation.

We consider that the mechanical relaxation possibly relate to the solvent transportation from gels, namely it is thought that relaxation of the compression load was induced by squeezing water from the gel. Since water is incompressible, the gels may maintain their volume when they are rapidly compressed. In this time, a load may be generated to maintain the volume. However, the solvent is squeezed out at a certain rate based on the friction between the solvent and the microscopic structure (in this case, it may be the network

structure). As shown in fig.6 and tables, τ_M and τ_V are almost coupled, although τ_M is somewhat smaller that τ_V for entire samples. However, since the values of the standard deviation were somewhat large, it is considered that the mechanical relaxation and the solvent transportation are qualitatively coupled. An interesting study on the force relaxation of poly (acrylic acid) hydrogels under compression (Kneable and Lequeux 1998) supports this hypothesis. They observed the quasi-exponentially decay of the compression force when compressed gels were immersed in aqueous medium. However, the compression force never changed when the gels were immersed in oils. These results means that the compression force relaxes as a result of the solvent transportation (squeezed out). Clearly, it is possible that defects may occur in the network structure during compression, and these defects may cause mechanical relaxation. However, because the applied strain was very small ($\gamma = 0.05$), it is proposed that the main cause of the mechanical relaxation was outflow of the solvent.

We should consider the friction between the solvent and the network structure to solve such a problem. Doi (1990) proposed the stress-diffusion coupling theory (SDCT), which is a continuum theory describing the deformation and solvent transport during the swelling of gels. The solvent transportation behavior of a cylindrical gel was studied by using SDCT (Yamane and Doi 2005). The result of the theoretical study shows that the transportation of the solvent follows a single exponential type function. However, we have to employ a stretched exponential function (Eq. 3 and 4) to analyze the experimental results precisely. It means that the relaxation mode is multiplex in this case, though it is impossible to know the details of each relaxation mode. Since reported SDCT studies only treat chemical cross-linked gels, they should not consider the change of the cross-linking structure. However, physical gels may change their network structure by thermal fluctuation or mechanical deformation. Such fluctuation of the network structure may affect the multiplicity of the relaxation mode. Therefore, it is difficult to completely explain the observed phenomena with SDCT.

The effect of the quenching temperature on the solvent transportation is also interesting. The characteristics of agarose gels vary depending on the cooling conditions, i.e., the gel forming process is a non-equilibrium process. For example, variation of the melting temperature of the gel depending on the sample preparation conditions has been reported (Mohammed et al 1998). It is well known that the sol-gel coexistence curve is upwardly convex in the concentration–temperature phase diagram of aqueous agarose solution. When the gels are prepared at the vicinity of the curve (the temperature just below the sol-gel coexistence temperature at a certain concentration), spinodal decomposition is observed (Morita et al 2013). That is, concentration fluctuation occurs in the agarose gels prepared at such temperatures, and formation of the network structure occurs in the condensed phase. On the other hand, when the hot solution is quenched at a far lower temperature, it is believed that the network structure grows from random nucleation without inducing concentration fluctuations. As described in the Results section, peaks are observed in the small angle scattering profile or there is an increase in the turbidity and an increase in the solvent transport rates for the sample quenched near the T_{gel}. These phenomena are attributed to micro-phase separation by

spinodal decomposition.

Conclusion

The relaxation behavior of the compression load and the volume change of compression constrained agarose gels were investigated. Simultaneous de-swelling and relaxation of the compression load was observed for the constrained agarose gel. Because the solvent transportation behavior during de-swelling could be analyzed by using an exponential type function, it is proposed that the de-swelling can be explained by the stress-diffusion coupling theory. Furthermore, it is considered that relatively large solvent flow pathways are present in the gels quenched at the victim of the T_g due to micro-phase separation by spinodal decomposition. This finding suggests that the solvent transportation from agarose gels can be controlled without the use of chemical additives, which is a valuable attribute for controlling flavor release of gelled food products.

Acknowledgement

This work was supported by JSPS KAKENHI Grant Number 25410231

References

Amici E, Clark AH, Normand V, Johnson NB (2002) Interpenetrating network formation in agarose - κ-carrageenan gel composites. Biomacromolecules 3:466-474.

Arnott S, Fulmer A, Scott WE, Dea ICM, Moorhouse R, Rees DA (1974) The agarose double helix and its function in agarose gel structure. J. Mol. Biol 90:273-284.

Boral S, Bohidar HB (2009) Hierarchical structure in agarose hydrogels. Polymer 50: 5585-5588.

Doi M (1990) Dynamics and Patterns in Complex Fluids. Onuki A and Kawasaki K (eds), Springer, Berlin pp100.

Fatin-Rouge N, Milon A, Buffle J, Goulet RR, Tessier A (2003) Diffusion anf partitioning of solutes in agarose hydrogels: The relative influence of electrostatic anf specific interactions. J. Phys. Chem. B 107: 12126-12137.

de Gennes P-G (1979) Scaling Concepts in Polymer Physics. Cornell University Press.

Hanazaki Y, Ito D, Furusawa K, Fukui A, Sasaki N (2013) Change in viscoelastic properties of agarose gel by HAp precipitation by osteoblasts cultured in an agarose gel matrix. J. Biorheology 26: 21-28.

Kneabel A, Lequeux F (1998) Force relaxation of single spherical gel beads under compression. Polymer Gels and Networks 5: 577-584

Mohammed ZH, Hember MWN, Richardson RK, Morris ER (1998) Kinetics and equilibrium processes in the formation and melting of agarose gels Carbohydrate Polymers 36: 15-26.

Morita T, Narita T, Mukai S, Yanagisawa M, Tokita M (2013) Phase behaviors of agarose gel AIP Advances3: 042128.

Morris VJ (1998) Gelation of polysaccharide in Functional properties of food macromolecules (Ed. Hill SE, Ledward DA, Mitchell JR). Aspen Publication. pp148

Nakamura K, Shinoda E, Tokita M (2001) The influence of compression velocity on strength and structure for gellan gels. Food Hydrocolloids 15: 247-252.

Nordqvist D, Vilgis TA (2011) Rheological study og gelation process of agarose-based solution. Food Biophysics 6: 450-460.

Russ N, Zielbauer B I, Koynove K, Vilgis TA (2013) Influence of nongelling hydrocolloids on gelation of agarose. Biomacromolecules 14: 4116-4124

Stieger M, van de Velde F.(2013) Microstructure, texture and oral processing: New ways to reduce sugar and salt in foods. Cur. Opin. Colloid & Intr. Sci. 18:334-348.

Suzuki A, Hara T (2001) Kinetics of one-dimensional swelling and shrinking og polymer gels under mechanical consraint. J. Chem. Phys. 114: 5012-5015.

Takahashi S, Kaneda I (2014) A transient network structure in sucrose stearate/water systems.Nihon Reoroji Gakkaishi 42: 103-109.

Tanaka T, Fillmore D (1979) Kinetics of swelling gels. J. Chem. Phys. 70:1214-1218.

Tokita M, Tanaka T (1991) Friction coefficient of polymer networks of gels. J. Chem. Phys. 95: 4613-4619.

Wang Z, Yang Y, Brenner T, Kikuzaki H, Nishinari K (2014) The influence of agar gel texture on sucrose

release. Food Hydrocolloids 36: 196-203.

Watase M, Nishinari K (1983) Rheological properties of agarose gels with different molecular weights.Rheol. Acta, 22: 580-587.

Yamane T, Doi M (2005) The stress diffusion coupling in the swelling dynamics of cylindeical gels. J. Chem. Phys. 122, 084703.

Table 1 Characteristic parameters of the compression load relaxation, analyzed using Eq. 3

Sample	L_0 [N]	τ_M [s]	α	L_r [N]
10-G	1.34 ± 0.102	94.0 ± 29.0	0.407 ± 0.0542	0.875 ± 0.0680
20-G	1.22 ± 0.179	97.7 ± 15.5	0.374 ± 0.0639	0.851 ± 0.0306
30-G	1.36 ± 0.0971	85.2 ± 19.6	0.372 ± 0.0270	0.856 ± 0.0448
35-G	1.21 ± 0.0947	40.2 ± 11.2	0.363 ± 0.0442	0.708 ± 0.0285
37-G	1.04 ± 0.0722	37.0 ± 2.44	0.407 ± 0.0542	0.623 ± 0.0515

Standard deviation is given as errors

Table 2 Characteristic parameters of the solvent transportation behavior, analyzed using Eq. 4

Sample	$V_0 \times 10^2$ [-]	τ_V [s]	β	$V_r \times 10^2$ [-]
10-G	2.69 ± 0.191	167 ± 59.6	0.460 ± 0.0971	97.2 ± 0.165
20-G	2.83 ± 0.719	147 ± 46.5	0.383 ± 0.0827	97.5 ± 0.218
30-G	2.88 ± 0.391	103 ± 55.9	0.397 ± 0.0855	97.4 ± 0.256
35-G	2.64 ± 0.528	63.5 ± 29.6	0.441 ± 0.0695	97.7 ± 0.288
37-G	3.65 ± 0.857	41.9 ± 21.1	0.369 ± 0.0804	96.6 ± 0.336

Standard deviation is given as errors

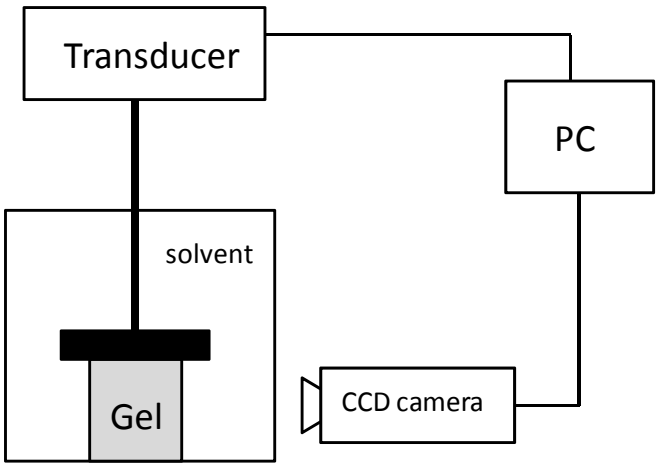

Fig. 1. Block diagram of the experimental apparatus for mechanical property and volume change analysis.

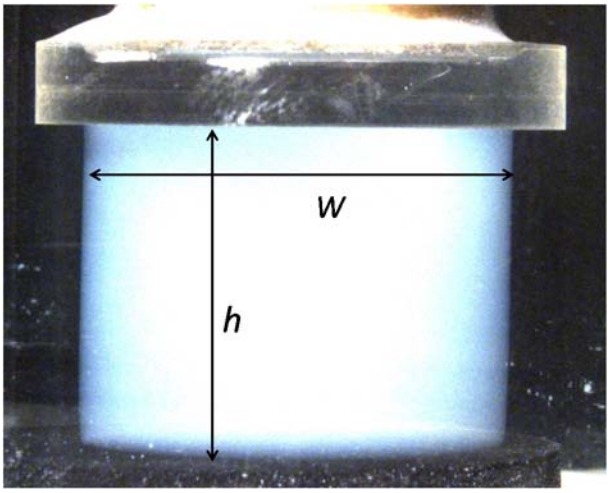

Fig. 2 Side view of the constrained agarose gel taken with a CCD camera (see Fig.1).

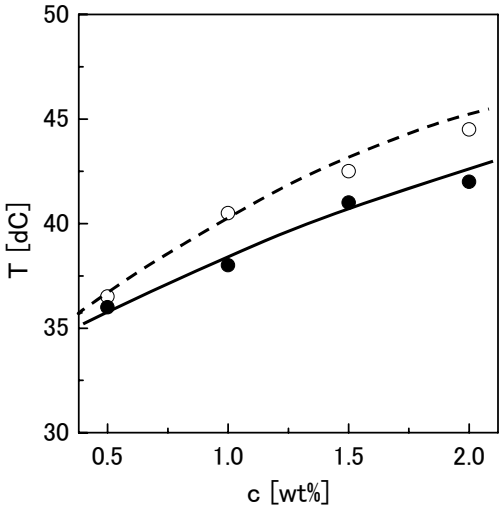

Fig. 3 Phase diagram for agarose/water system, obtained during cooling process. Open circles and closed circles denote the cloud temperature and sol-gel coexisting temperature, respectively.

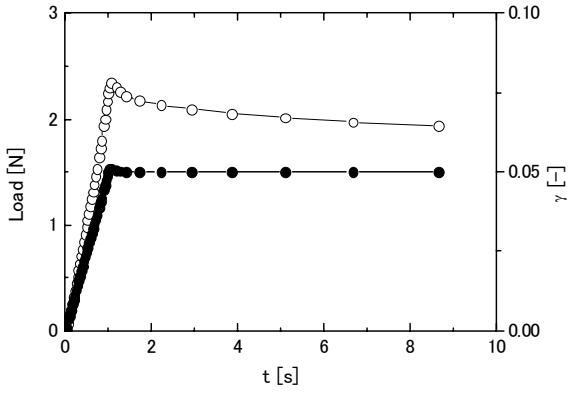

Fig. 4 Time development of the compression load and compression strain for 10-G; sample was compressed at a speed of 1 mm/s until a strain of 0.05 was achieved, followed by constraint at $\gamma = 0.05$. Open circles and closed circles denote the compression load and the compression strain, respectively.

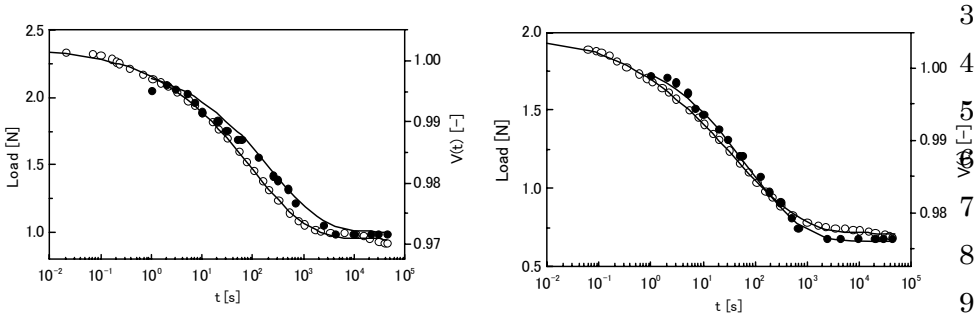

Fig. 5 Plots of temporal variation of the compression load (open circles) and the volume change (closed circles) for sample 10-G (a: the left plate) and 37-G (b: the right plate). The lines show the best fit results of the analysis with Eqs. 3 and 4.

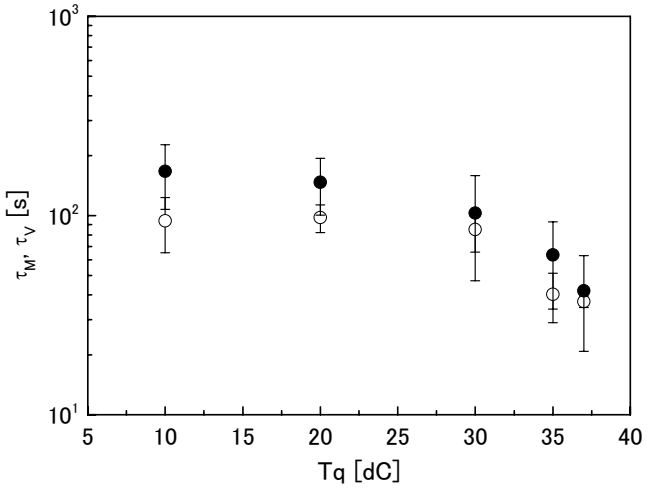

Fig. 6 Dependence of time constants on quenching temperature. The open circles and closed circles denote τ_M and τ_V, respectively. The error bars show the standard deviation.

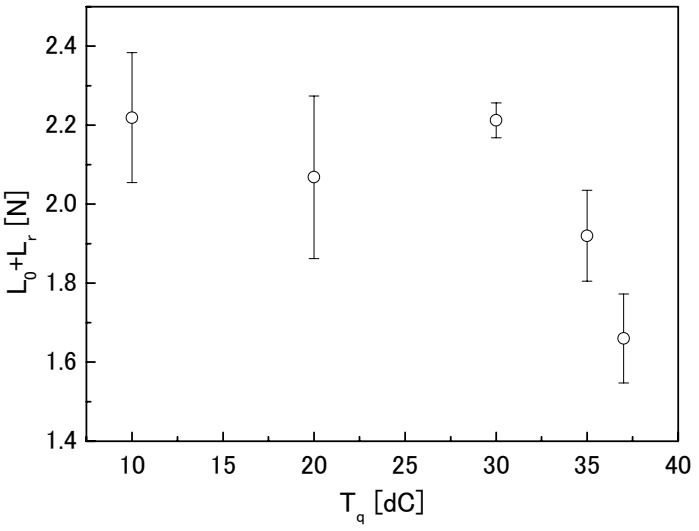

Fig. 7 Quenching temperature dependence of (L_0 + L_r), i.e., the instantaneous load at γ = 0.05. The error bars show the standard deviation.

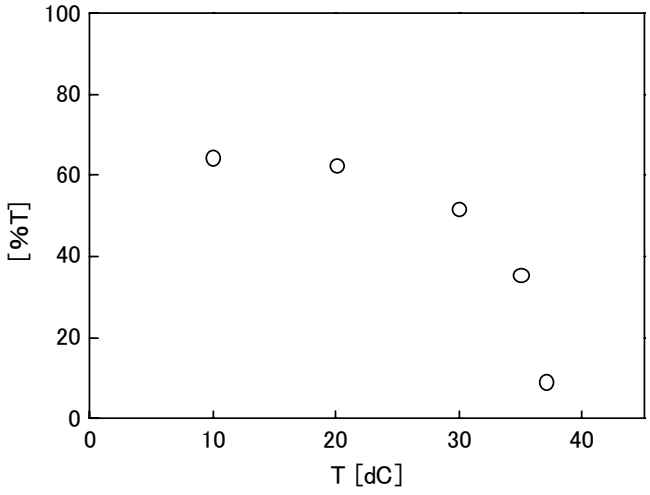

Fig. 8 Dependence of turbidity of gels on quenching temperature; the turbidity was quantified as the transmittance at λ = 540 nm.

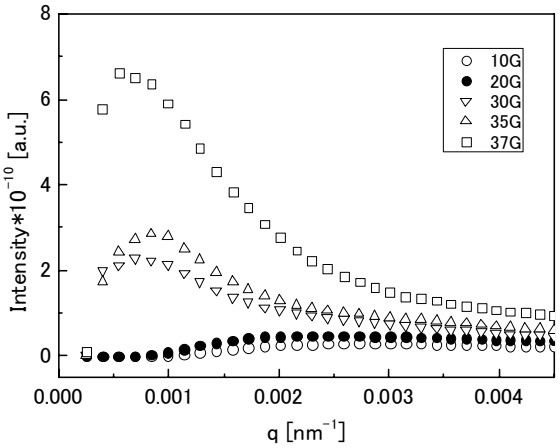

Fig. 9 Small angle light scattering profiles of gels.